

Emission lines and optical continuum in low-luminosity radio galaxies

K.A. Wills¹, R. Morganti², C.N. Tadhunter¹, T.G. Robinson¹, M. Villar-Martin³

¹ *Department of Physics and Astronomy, University of Sheffield, Hounsfield Road, Sheffield, S3 7RH, UK*

² *Netherlands Foundation for Research in Astronomy, Postbus 2, 7990 AA Dwingeloo, The Netherlands*

³ *Department of Physical Sciences, University of Hertfordshire, College Lane, Hatfield, Herts AL10 9AB, UK*

ABSTRACT

We present spectroscopic observations of a complete sub-sample of 13 low-luminosity radio galaxies selected from the 2Jy sample. The underlying continuum in these sources is carefully modelled in order to make a much-needed comparison between the emission line and continuum properties of FRIs with those of other classes of radio sources. We find that 5 galaxies in the sample show a measurable UV excess: 2 of these sources are BL Lacs and in the remaining 3 galaxies we argue that the most likely contributor to the UV excess is a young stellar component. Excluding the BL Lacs, we therefore find that $\sim 30\%$ of the sample show evidence for young stars, which is similar to the results obtained for higher luminosity samples. We compare our results with far-infrared measurements in order to investigate the far-infrared-starburst link. The nature of the optical-radio correlations is investigated in light of this new available data and, in contrast to previous studies, we find that the FRI sources follow the correlations with a similar slope to that found for the FRIIs. Finally, we compare the luminosity of the emission lines in the FRI and BL Lac sources and find a significant difference in the [OIII] line luminosities of the two groups. Our results are discussed in the context of the unified schemes.

Key words:

galaxies: active – galaxies: individual – galaxies: emission lines – quasar: general

1 INTRODUCTION

Following the work of Fanaroff & Riley (1974), it is now well understood that extended radio galaxies appear to come, broadly speaking, in two different flavours: edge-darkened, low radio power and powerful ($> 2.5 \times 10^{26}$ W Hz⁻¹ at 178 MHz; Baum, Zirbel & O’Dea 1995), edge-brightened. The former are usually known as Fanaroff-Riley type I (FRI) and the latter as Fanaroff-Riley type II (FRII). However, the nature of this dichotomy remains unclear: whether this is related to the nature of the nuclear engine (perhaps the black-hole mass or spin), the mass accretion rate, or even on a larger scale the conditions of the ISM.

Resolving this issue requires knowledge of the characteristics of the emission (in different wavebands) from both types of radio galaxies; understanding the mechanisms that may produce the emission and explaining the differences. A number of studies have recently concentrated on understanding the nuclear characteristics of FRIs using optical data. From HST observations, the presence of an optical non-thermal component has been confirmed by the detection of central compact cores (CCCs) in HST images of FRIs

(Chiaberge, Capetti & Celotti 1999). The correlation between the CCC’s optical flux and the flux of the radio core for FRI/BL Lacs objects (Chiaberge et al. 1999) indicates that these cores are due to optical synchrotron radiation produced in the inner region of a relativistic jet. This is therefore consistent with the idea that FRIs are the parent population of the BL Lacs, as predicted by the unified schemes (Urry & Padovani 1995). Moreover, the detection of optical cores in a large fraction of FRI radio galaxies suggests that the circumnuclear disks, if present, must be geometrically thin, unlike the optically and geometrically thick tori which are an essential ingredient of the unified schemes for powerful FRIIs/radio-loud quasars. This already points to some, possibly intrinsic, difference in the nuclear regions of FRI and FRII radio galaxies.

Another powerful indicator of the activity in the nucleus is the warm ionised gas in the circumnuclear regions. This can be studied using the optical emission lines, and indeed has been extensively used in FRII to test the unified schemes hypothesis and to understand the ionization mechanism for the gas. Partly as a result of the low luminosity of their emission lines, only sparse spectroscopic data are

arXiv:astro-ph/0310256v1 9 Oct 2003

available for the FRIs. Compared to FRIIs, FRIs have (on average) 5 to 30 times weaker emission lines (for a similar radio total luminosity, Baum et al. 1995). This has therefore limited the study of the characteristics of these galaxies. Indeed, FRIs are invariably classified as weak-line radio galaxies (WLRG). A tight correlation between radio core emission and $H\alpha + [\text{NII}]$ emission in FRIs has recently been confirmed by Verdoes Kleijn et al. (2002) using HST narrow band images. This has been interpreted as a strong indication that the emission gas is excited by an AGN-related process and not only due to processes associated with the host galaxy (e.g. old stars).

An interesting ‘complication’ is the suggestion that FRIs and FRIIs follow separate correlations between optical line luminosity and radio luminosity (Baum et al. 1995). However, from this published data it is not clear the extent to which this is really the case and in a later paper, Tadhunter et al. (1998) argue that only the $[\text{OIII}]$ correlation, and not the $[\text{OII}]$ correlation, indicates a difference between FRI and FRII sources. It is important to point out, however, that the Tadhunter et al. study, although based on a well-defined sample, resulted in many upper limits in the data. Part of the problem with previous studies has been the lack of accurate continuum subtraction, which is essential for measuring accurate fluxes and upper limits for the faint emission lines present in the spectra of FRI sources. Therefore, in order to advance our understanding of the FRI sources further, it is important to make higher quality observations of a well-defined sample and also to model and subtract the underlying continuum emission.

The analysis of the optical continuum is itself an important component in understanding the characteristics of FRIs relative to FRIIs. Much progress has already been made in analysing the optical continua of powerful FRII radio galaxies, particularly in understanding the nature of the UV excess that is often present in these galaxies (Tadhunter, Dickson & Shaw 1996, Robinson et al. 2000, Aretxaga et al. 2001, Wills et al. 2002, Tadhunter et al. 2002). These studies suggest that approximately 30% of the observed host galaxies of FRIIs show a significant contribution from a young stellar population component — probably related to starbursts induced in the merger events which triggered the activity. However, no systematic studies have been done for FRI sources, although at least one FRI is known to have a young stellar component (Melnick, Gopal-Krishna & Terlevich 1997, Aretxaga et al. 2001), and a significant fraction of FRIs are also known to exhibit UV continuum excess (e.g. Tadhunter et al. 2002). Clearly, in order to investigate whether the triggering events are similar in the two types, it is important to compare the optical/UV continuum properties of the FRI and FRII host galaxies. Again, such studies have been hampered in the past by the poor quality of the optical data for the FRI sources.

Here we present new, high quality optical spectra collected for a complete sub-sample of 13 low-luminosity radio galaxies selected from the Tadhunter et al. (1993, 1998) sample of 2Jy radio sources. These data increase substantially the number of FRIs for which good quality spectra are available, and they allow us to compare the emission line and continuum properties of the FRIs with those of other classes of radio sources such as FRIIs and BL Lacs.

A Hubble constant of $H_0 = 50 \text{ km s}^{-1} \text{ Mpc}^{-1}$ and a deceleration parameter of $q_0 = 0$ are assumed throughout.

2 THE OBSERVATIONS

The sample chosen for the purposes of this study comprises all objects with FRI or core/halo radio morphologies, or classified as BL Lac objects from the complete sample of 2Jy radio sources described in Tadhunter et al. (1993, 1998), with RAs in the range $04\text{h} < \text{RA} < 17\text{h}$ (with the exception of Cen A). Some general properties of this sample are listed in Table 1. Most of the 14 sources in the sample fall at the lower end of the radio power range for the 2Jy sample, and all of the objects are at relatively low redshifts ($z < 0.06$). Spectroscopic observations for thirteen galaxies (excluding 0521-36 because of a lack of time) were obtained with the EFOSC2 at the ESO/MPG 2.2m telescope in February 1996.

The observations were carried out using a Thomson THX31156 1024×1024 CCD with $19 \mu\text{m}$ ($0.33''$) pixels, a 2 arcsecond slit and Grism #3. The Thomson chip has a gain of $2 e^-/\text{ADU}$ and the readout noise is less than $5 e^-$ rms. Use of Grism #3 at an effective blaze of 3900 \AA resulted in a dispersion of $1.9 \text{ \AA pixel}^{-1}$ and an approximate wavelength coverage of $3500\text{--}5400 \text{ \AA}$. The instrumental resolution was $\sim 9.0 \text{ \AA}$ with the 2 arcsecond slit. For each source, the observations consisted of between two and four cycles of typically 1200s per cycle (occasionally 300s, 600s or 900s cycles were used). This resulted in a total of nearly 11 hours integration time for the 13 radio galaxies. All but one of the sources were observed at relatively low airmass (typically < 1.1 , but three sources 1.15–1.25). Note that the source with the highest airmass (1514+07, 1.33) shows a relatively poor fit in the red region of the spectrum, probably as a result of differential refraction (see §3.4).

Reduction of the data proceeded along conventional lines using the Starlink FIGARO package. This involved bias subtraction, cosmic ray removal, flat-field correction, wavelength calibration, atmospheric extinction correction, flux calibration and sky subtraction. Flat-field correction was undertaken using dome flats acquired with a 2 arcsec slit. Flux calibration was provided via observations of the spectrophotometric standard stars EG 54, 76 and 248 using a 5.0 arcsec slit. Comparison between these different standard star observations gives a relative flux calibration error of ± 7 per cent across the wavelength range of each galaxy.

A typical extraction aperture of 2 arcsec (slit width) \times 7.1 arcsec (21 pixels) was used in order to provide full coverage of the nuclear regions of each source. The final rest-frame intensity spectra are shown in Figure 1 (see Table 1 for redshifts used in the shift to the rest-frame). The wavelength range of these spectra are equivalent to the observed wavelength range $3500 - 5400 \text{ \AA}$, except in the case of 0453-20 and 0620-52 where the observed wavelength range has been cropped to $3700 - 5400 \text{ \AA}$ due to light leakage on to the blue region of the CCD. The spectra have been corrected for the effects of galactic reddening using the Seaton (1979) extinction curve and the values of $E(B-V)$ derived from the full-sky dust map presented in Schlegel, Finkbeiner & Davis (1998, see Table 1). We have also subtracted the nebular continuum (see Dickson et al. 1995) in the case of 1514+07

Table 1. Details of the radio galaxies in the sample. Column 3 gives the redshifts which are taken from either Tadhunter et al. 1993 (\dagger), our own spectra (\ddagger) or the NASA/IPAC Extragalactic Database (NED) (*), depending on which value gives the best fit to the continuum (see also §3.4). The 4.8 GHz radio power (total and core) are taken from Morganti, Killeen & Tadhunter (1993) and the morphological classification comes from the images in Morganti et al. (1993, 1999) (I = FRI, C+D = core + diffuse emission, CJ = core/jet). VLBI images of some of the sources are also presented in Venturi et al. (2000). The $R_{2.3\text{GHz}}$ parameter (column 7) is defined as $R = S_{\text{core}}/(S_{\text{tot}} - S_{\text{core}})$ and comes from Morganti et al. (1999). The E(B-V) values for galactic reddening have been derived from the full-sky dust map presented in Schlegel, Finkbeiner & Davis (1998).

Name		z	Radio Morphology	log P _{tot} W/Hz	log P _{core} W/Hz	R _{2.3GHz}	E(B-V) mag.
0427-53		0.0412*	I	25.33	23.56	0.0169	0.012
0453-20	OF-289	0.035 \dagger	I	24.99	23.34	0.112	0.041
0521-36		0.055 \dagger	CJ	26.10	25.28	0.176	0.038
0620-52		0.051 \dagger	I	25.17	24.49	0.062	0.068
0625-35	OH-342	0.0525 \ddagger	I	25.46	24.91	0.227	0.067
0625-53		0.0556 \ddagger	I	25.40	23.75	0.0078	0.094
0915-11	Hydra A	0.0542 \ddagger	I	26.26	24.46	0.0067	0.042
1216+06	3C 270	0.00747*	I	24.16	22.69	0.0194	0.018
1246-41	NGC4696	0.00994 \ddagger	C+D	23.68	21.81	0.0068	0.113
1251-12	3C 278	0.0157 \ddagger	I	24.39	22.94	0.016	0.053
1318-43	NGC 5090	0.0117 \ddagger	I	23.97	23.49	0.153	0.144
1333-33	IC 4296	0.013 \dagger	I	24.67	23.34	0.019	0.062
1514+07	3C 317	0.034 \ddagger	C+D	24.73	24.34	0.163	0.037
1514-24	ApLib	0.0480 \ddagger	CJ	25.29	25.17	34	0.138

and Hydra A, since these two are the only galaxies within our sample to show a measurable H β component.

In addition to our observations of the 13 radio galaxies, we also present the results for the source 0521-36 (which we were unable to observe due to time constraints) taken from Tadhunter et al. (1993) and Boisson, Cayatte & Sol (1989) for completeness.

3 RESULTS

We have used the extracted spectra (Figure 1) to derive both the luminosity of the emission lines and the characteristics of the continuum. The latter gives information on the presence of a possible UV excess and on the stellar population. As in the previous studies carried out on powerful radio galaxies (Wills et al. 2002, Tadhunter et al. 2002), we combine two different approaches to investigate the possible presence and origin of a UV excess. We first measured the 4000 Å break and then performed a more detailed fit to the continuum. Furthermore, by subtracting the best-fit to the continuum of the spectra, we were able to detect emission lines otherwise too weak to be seen.

3.1 4000 Å break measurement

A way to quantify the UV excess is to measure the 4000 Å continuum break (D(4000), Bruzual 1993). This is prominent in the spectra of evolved stellar populations and therefore characterises the large decrease, by a factor of ~ 2 in the flux below 4000 Å, in the continuum emission of early-type galaxies. In line with our previous work on powerful radio galaxies, we modify the bins used by Bruzual to precisely

define D'(4000), in order to avoid emission line contamination, and instead use the ratio of the total flux in a bin 100 Å wide centred on 4200 Å (rest frame) to the total flux in a bin of identical width centred on 3800 Å. Using this modified definition, we can calculate that elliptical galaxies with solar metallicity and ages of 10 and 15 Gyr have values of D'(4000) of approximately 2.1 and 2.3 respectively, and so any value significantly less than these is indicative of an additional blue component. In Table 2 we show the D'(4000) values for the sample.

Of the 13 observed radio galaxies, 8 have D'(4000) > 2.0 but for 5 other galaxies the values are significantly less than this, indicating the presence of an additional blue component. For example, Ap Lib shows a very low value of D'(4000), consistent with it being a BL Lac. However, note that a low value of D'(4000) alone is not sufficient to classify a source as a BL Lac and instead the classification of BL Lacs from our sample needs to be made on an individual basis.

3.2 Continuum modelling

To learn more about the nature of the optical continua in the sources, we have also modelled the continua using the results of published isochrone spectral synthesis models. The modelling of the continuum was carried out using the method already described in previous papers (e.g. see Tadhunter et al. 1996, Robinson et al. 2000, Wills et al. 2002). To model the continuum spectral energy distributions (SEDs) of each galaxy we use the intensity spectra shown in Figure 1 (in the observed wavelength range 3400 to 5400 Å, except for 0453-20 and 0620-52 where the observed wavelength range has been cropped to 3700 - 5400 Å), which have been corrected

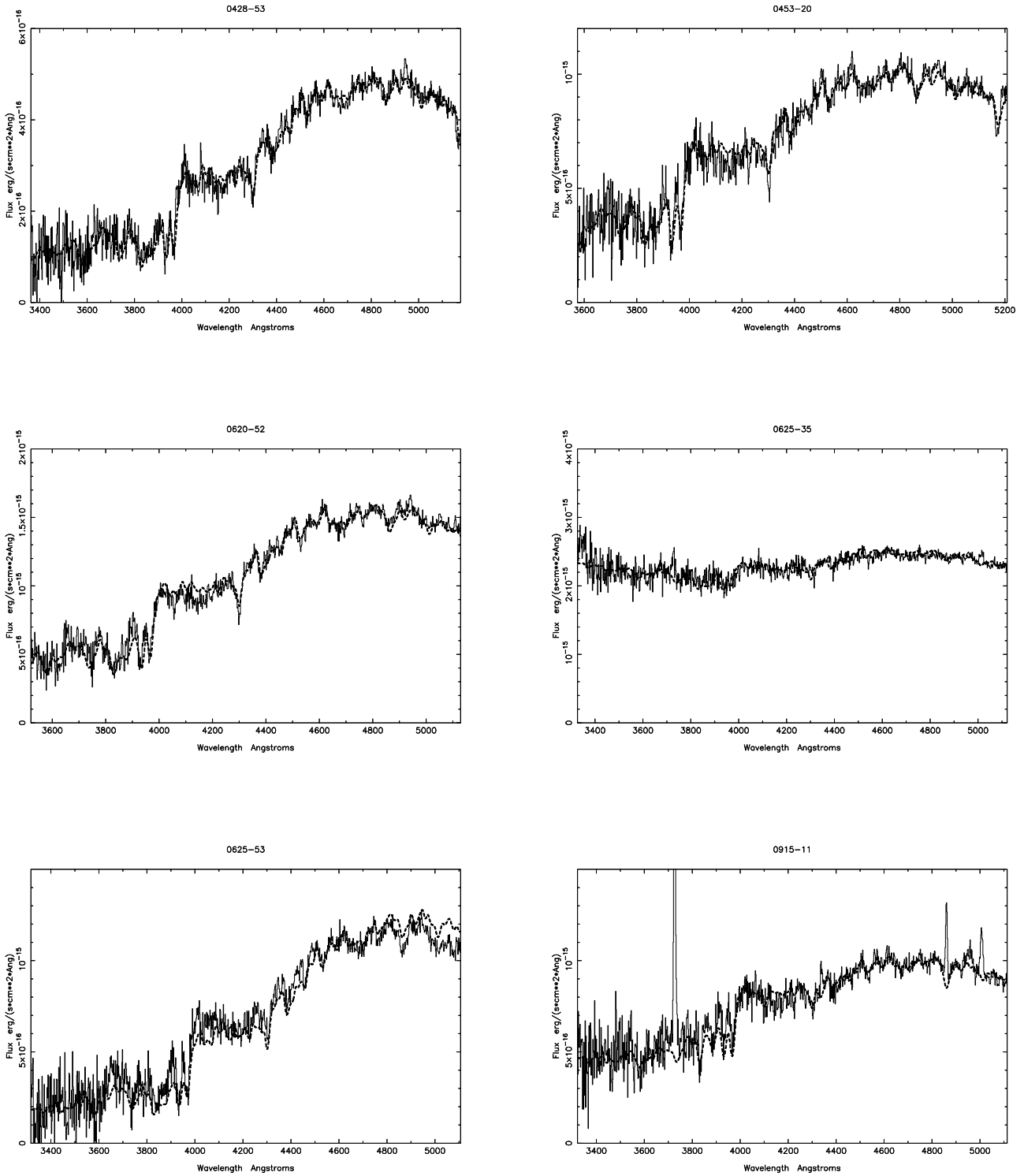
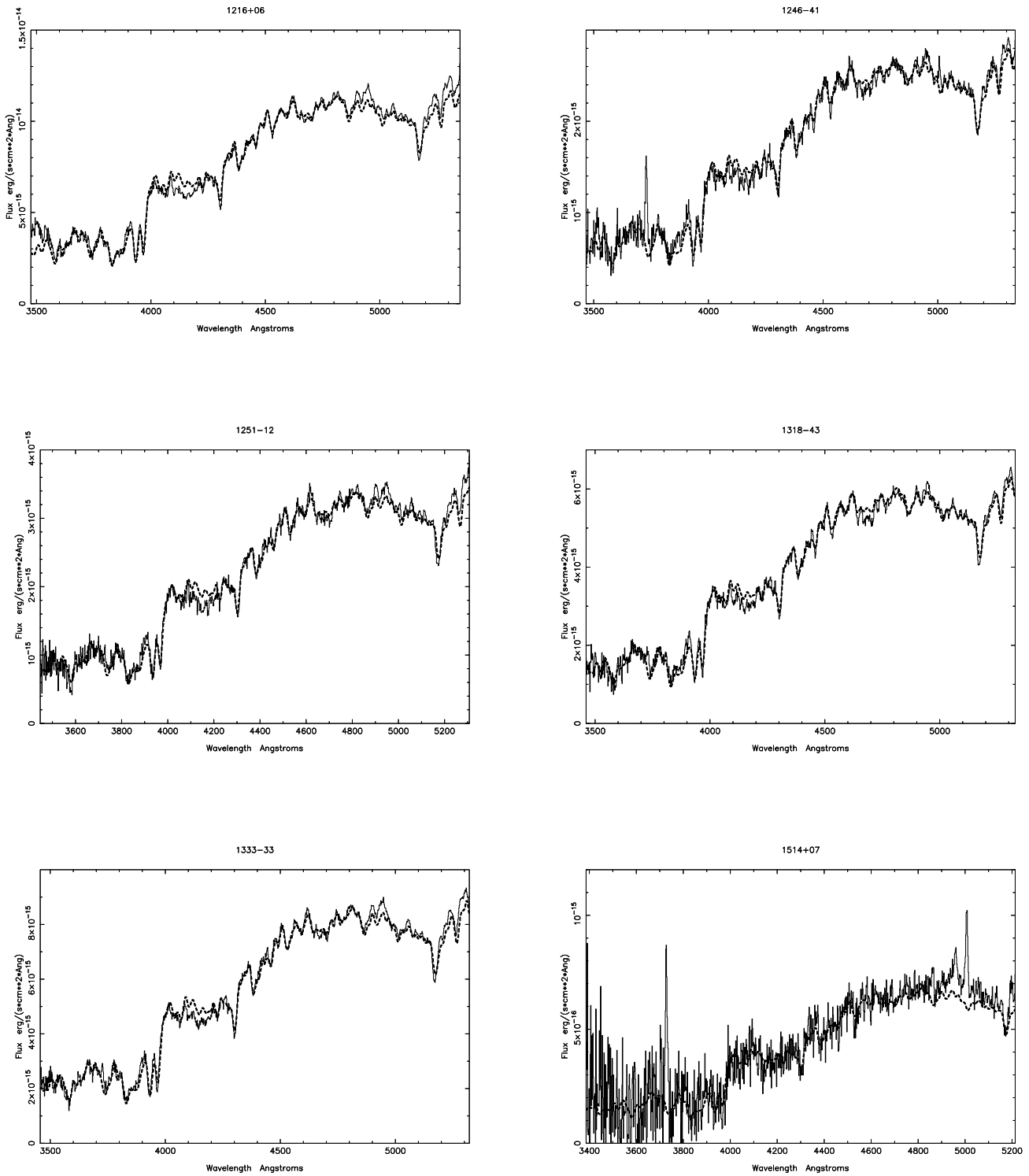


Figure 1. The rest frame intensity spectra of the 13 observed radio galaxies in the sample following nebular continuum subtraction (in the cases of 1514+07 and Hydra A) and a correction for galactic reddening (thin solid line) and the best-fitting one- or two-component model (thick dotted line). See text and Table 3 for further details.



v

Figure 1. cont.

Table 2. Measurements of the 4000 Å break (see §3.1), the flux and luminosity of the emission lines (see §3.3) and the far-infrared flux and luminosity (see §3.5) for the galaxies in the sample. In the cases where the [OII] and [OIII] flux are both quoted as upper limits, we do not calculate a [OIII]/[OII] ratio since its value is not particularly meaningful. We quote the values for 0521-36 from Tadhunter et al. (1993) where available. The far-infrared fluxes and luminosities quoted have been calculated by co-adding scans from the IRAS ‘all-sky’ survey (see §3.5 for full details) except in the cases (marked (P)) for which ‘pointed observations’ are available (Golombek, Miley & Neugebauer 1988; Impey & Neugebauer 1988). All luminosities have been calculated assuming $H_0 = 50 \text{ km s}^{-1} \text{ Mpc}^{-1}$ and $q_0 = 0$.

Name	$D'(4000)$	$\log F_{[\text{OII}]}$ $\text{ergs}^{-1}\text{cm}^{-2}$	$\log F_{[\text{OIII}]}$ $\text{ergs}^{-1}\text{cm}^{-2}$	$\log L_{[\text{OII}]}$ ergs^{-1}	$\log L_{[\text{OIII}]}$ ergs^{-1}	[OIII]/[OII]	F (60 μm) mJy	log L (60 μm) W/Hz
0427-53	2.04	<-14.98	<-15.46	<39.91	<39.42	-	< 48	< 23.5
0453-20	1.82	<-14.64	<-15.31	<40.10	<39.43	-	690	24.5
0521-36	-	-14.49	-13.99	40.66	41.16	3.13	354 (P)	24.6 (P)
0620-52	1.86	<-14.71	<-15.46	<40.37	<39.61	-	60	23.8
0625-35	1.06	-14.24	-14.46	40.86	40.64	0.59	60	23.8
0625-53	2.24	<-14.80	<-14.91	<40.31	<40.19	-	< 63	< 23.9
0915-11	1.43	-13.79	-14.42	41.34	40.71	0.24	155 (P)	24.2 (P)
1216+06	2.01	-14.12	<-14.43	39.26	<38.95	<0.49	< 156	< 22.5
1246-41	2.06	-13.95	-14.47	39.69	39.17	0.30	120	22.6
1251-12	2.09	-14.63	-14.71	39.41	39.33	0.83	< 111	< 23.0
1318-43	2.08	-14.14	<-14.60	39.64	<39.18	<0.35	160	22.9
1333-33	2.09	-14.09	<-14.43	39.79	<39.45	<0.46	130	22.9
1514+07	2.03	-14.14	-14.39	40.59	40.33	0.56	< 99	< 23.6
1514-24	1.18	<-13.88	-14.32	<41.14	40.70	>2.8	260 (P)	24.4 (P)

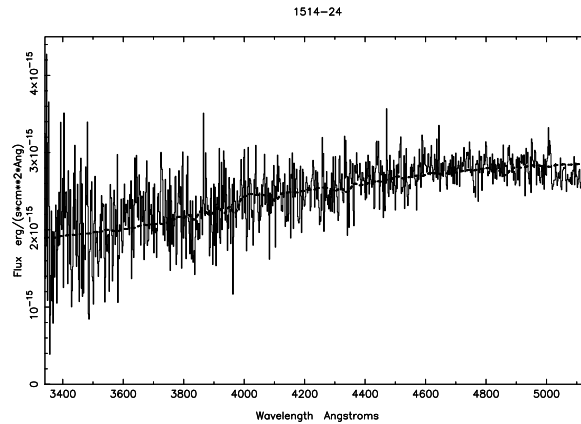


Figure 1. cont.

for galactic reddening and where applicable, had the nebular continuum subtracted. The continuum of each galaxy was initially modelled using two components chosen to represent AGN light and the light of the host elliptical galaxy. For the elliptical galaxy template spectrum we used the Bruzual & Charlot instantaneous burst models (see Leitherer et al. 1996) with Salpeter (1955) IMF, solar metallicity and age ranges from 15 to 10 Gyr. For the AGN light we use a power-law of the form $f_\lambda \propto \lambda^{+\alpha}$. We also tried incorporating a third component corresponding to a contribution from young stars, with the starburst age ranging from 0.05 - 5 Gyr. The models were generated by using a normalising continuum bin of 4806.3 - 4830.0 Å and scaling the differ-

ent model components such that the total model flux in the normalising bin was less than 125% of the observed flux. As a result a series of models were created and the best-fitting model was found using a reduced chi-squared test.

The results from this fitting are given in §3.4 and are summarised in Table 3. In addition we also quote the results from Boisson et al. (1989) for the fitting to the continuum of 0521-36. From the 14 sources in the sample we find that in 8 cases, we require only an old stellar population (10-15 Gyr) to fit to the continuum. In 3 cases (0453-20, 0620-52, 0915-11) an additional young population (0.05 - 2 Gyr) is also required in order to obtain a good fit to the continuum. In the 3 remaining cases, a power-law is required in order to

obtain a good fit (the three BL Lac type objects 0625-35, 0521-36 and 1514-24).

3.3 Emission Lines

The best fit to the continuum has been subtracted from the spectra in order to be able to identify the emission lines. This method allows detections of emission lines otherwise hidden by the strong thermal continuum. With the exception of Hydra A and 1514+07, we detected only (at most) [OII] and [OIII].

In the cases where both [OIII]4959 Å and [OIII]5007 Å lines are visible, the fit to these lines has been performed by: *i*) forcing the width of the [OIII]4959 Å and [OIII]5007 Å lines to be equal; *ii*) forcing their separation to be 48 Å; *iii*) forcing the intensity of the [OIII]5007 Å line to be 3 times the 4959 Å line. If only the [OIII]5007 Å line is visible we fitted to this as a single line. If a specific line is not visible, we have calculated 3σ upper limits to the flux and luminosity of that line, obtained from an 11 Å (the average linewidth) region. Table 2 lists the line fluxes, luminosities and line ratios as measured from the spectra. In addition we also quote the values for 0521-36 from Tadhunter et al. (1993) where available.

In 6 galaxies (0625-35, 1246-41, 1251-12 ([OII] and [OIII]); 1216+06, 1318-43, 1333-33 ([OII] only)) we detected emission lines when previously (Tadhunter et al. 1993) we had just upper limits. In 1514-24 we detect only [OIII], whereas in Tadhunter et al. both [OII] and [OIII] were weakly detected. Note that two out of the three objects which show a young stellar population component (the only exception being Hydra A) do not show strong emission lines (only upper limits could be given)

The model subtracted spectra are shown in Figure 2.

3.4 Notes on individual objects

In 8 out of 14 of the objects in our sample we find no evidence for a UV excess and instead, an old stellar population (10-15 Gyr) provides an adequate fit to both the general shape and the detailed absorption line features of the continuum spectra. For each of these objects, we can achieve a marginally improved fit to the continuum if we include a small contribution from a power-law component (typically <20% of the flux in the normalising bin). The luminosities of the required power-law components ($\log L$ (W/Hz) = 19.8-20.5 in the normalising bin) are consistent with those measured for the nuclear point source components detected by Chiaberge et al. (2002, $\log L$ (W/Hz) = 18.1-20.3) in HST images, albeit at the upper end of the range. However, the power-law slopes are redder (typically $\alpha > 4$) than measured in most of the Chiaberge et al. sources (typically $\alpha \sim 2.5$). Although we cannot rule out the possibility that we are detecting the nuclear point source components in our objects, an alternative possibility is that the putative power-law component is compensating for inadequacies in the flux calibration or the isochrone spectral synthesis models.

In 3 out of 14 of the objects in our sample we find evidence for a UV excess and require an additional young stellar component (0.05 - 2 Gyr) to obtain an acceptable fit to the continuum. For two of these objects (0453-20 and

0620-52) we find that the addition of a power-law component to an old stellar population is also able to produce a good fit to the continuum. However, the luminosities of the required power-law components ($\log L$ (W/Hz) = 20.6-21.1 in the normalising bin) are significantly larger than those of the point source components of Chiaberge et al. (2002). In any case, although the addition of the power-law component provides a good overall fit to the general shape of the continuum spectra, the fits to the continuum SED and in particular the detailed absorption line features, are significantly improved when the power-law component is replaced by a young stellar component. In the third object of this group (0915-11) the addition of a power-law component does not provide an adequate fit to the continuum, as is discussed in detail below.

In general, the models provide an excellent fit over most of the spectral range covered by the data. However, we note that in the rest frame wavelength range 4050 – 4200 Å, the models often show a significant excess relative to the data (see Figures 1 and 2). Since this excess is seen in the same rest wavelength range for objects covering a wide range in redshift, we suggest that the excess represents a problem with the models rather than with the flux calibration.

0427-53 This galaxy does not show a UV excess either from the 4000 Å break or from the fit to the continuum. The best fit was obtained by using a value of the redshift of $z=0.0412$ ($z=0.038$ previously quoted by Tadhunter et al. 1993) and with an old stellar population only (15 Gyr gives $\chi^2 = 1.44$). No emission lines were detected.

0453-20 This galaxy shows a UV excess (from D'). In the fit to the continuum, a definite improvement is seen by the addition of a young stellar component (e.g. χ^2 is ~ 3 for a 15 Gyr component only compared with ~ 0.6 for a 15 Gyr component plus a 0.05 Gyr component). The best fit is obtained with a 15 Gyr component plus a 0.05 Gyr component which fits very well except for a slight excess around 4100 Å ($\chi^2 = 0.597$). In addition, we also get good fits ($\chi^2 \sim 0.7$) with a 15 Gyr component plus a 0.1 Gyr component, or a 15 Gyr component plus a 2-5 Gyr component, or a 5 Gyr component only. No emission lines were detected.

0521-36 This source has an optically variable continuum which has resulted in its classification as a BL Lac object (see Danziger et al. 1979). Both Danziger et al. (1979) and Boisson et al. (1989) note that the optical SED of this source requires a strong power-law component with $\alpha \sim -0.5$, in addition to an elliptical galaxy component. Both the [OII] and [OIII] lines were detected by Tadhunter et al. (1993).

0620-52 This galaxy shows a UV excess. In the fit to the continuum, a definite improvement is seen by the addition of a young stellar component (e.g. χ^2 is ~ 2 for a 15 Gyr component only compared with ~ 0.7 for a 15 Gyr component plus a 2 Gyr component). The best fit is obtained with a 15 Gyr component plus a 2 Gyr component ($\chi^2 = 0.746$), but adequate fits ($\chi^2 \sim 0.8$) can also be obtained for young stellar components of ages 1-5 Gyr and 0.05-0.1 Gyr. This object was observed with the SAX satellite but has no obvious non-thermal component (Trussoni et al. 1999). No emission lines were detected.

0625-35 We suggest that this source could be a BL Lac object on the basis of the results of the 4000 Å break ($D'(4000)=1.06$) and from the fit to the continuum. It is not possible to gain an adequate fit to the continuum with

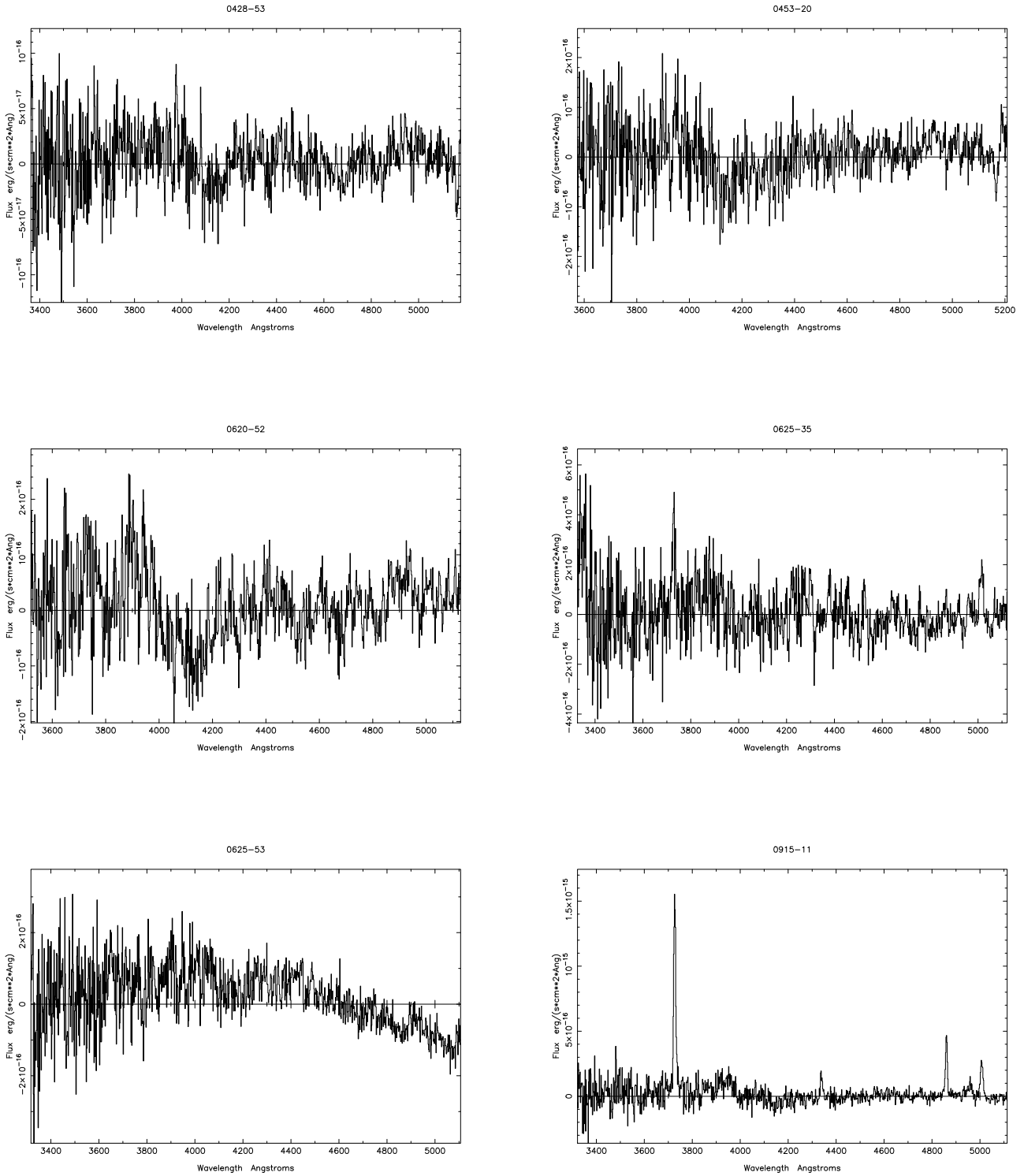


Figure 2. The rest frame model-subtracted spectra of the 13 observed radio galaxies in the sample. The best-fitting model for each galaxy, as detailed in Table 3, has been subtracted.

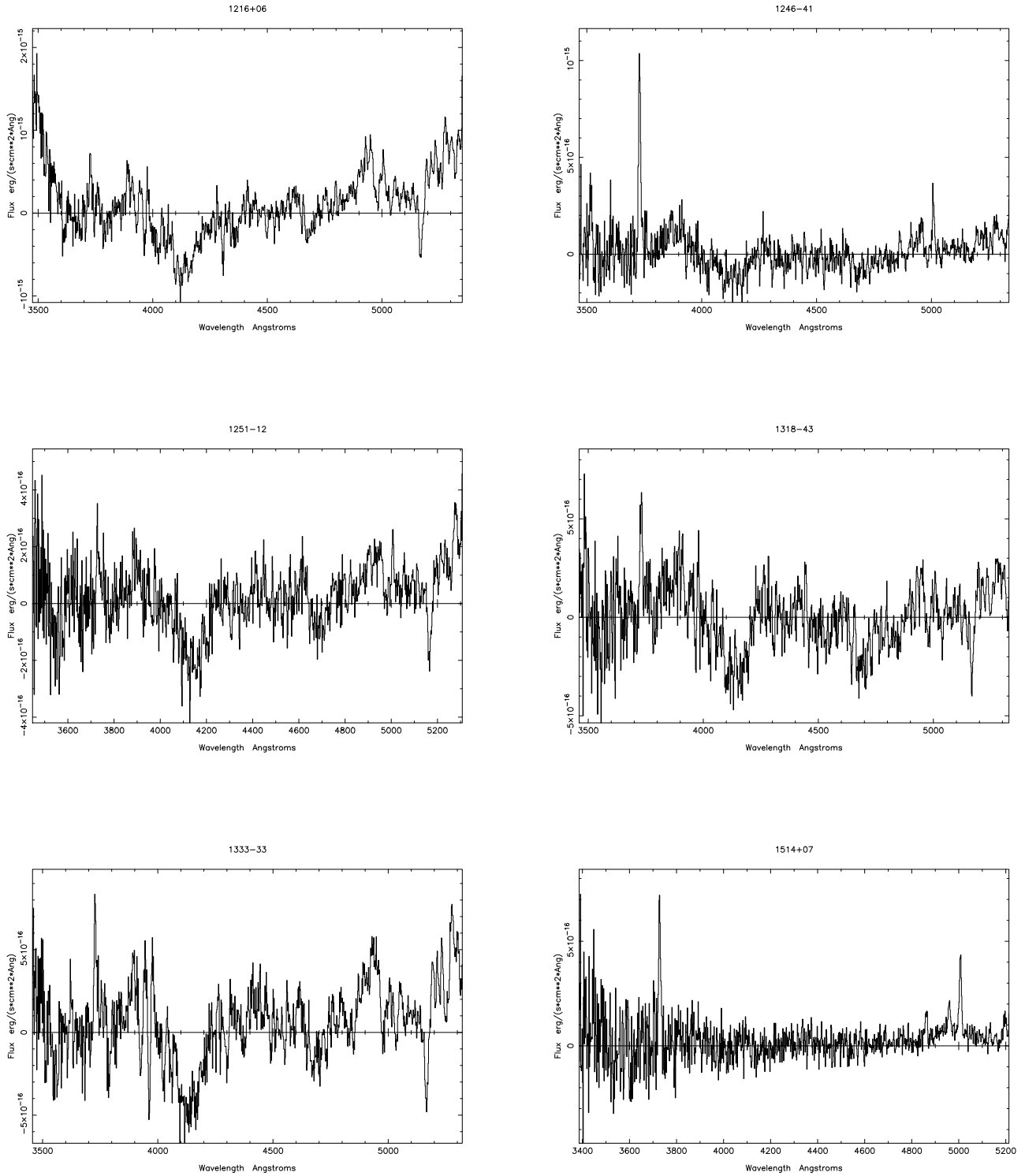


Figure 2. cont.

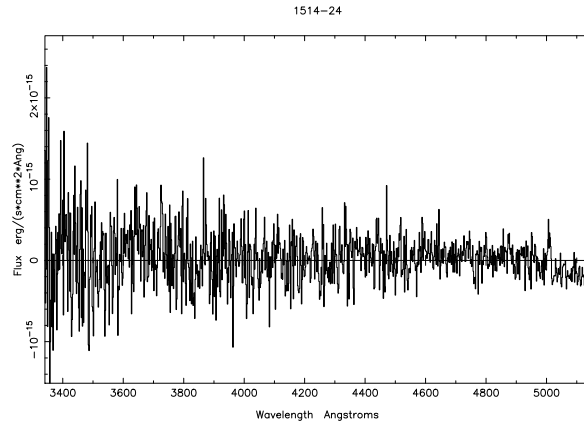


Figure 2. cont.

Table 3. The best-fitting models to the continuum for each galaxy in our sample. In the cases where more than one model is given, the first one is the one used in the figures and in the deduction of the emission line data. In many cases we actually find acceptable fits with a range of young and old stellar ages, of which the one shown is an example. More details are given in §3.4. The results for the modelling of the continuum of 0521-36 are given from Boisson et al. (1989).

Name	Best fit	χ^2
0427-53	15 Gyr (101.5%)	1.44
0453-20	15 Gyr (88.8%) + 0.05 Gyr (10.2%) 5 Gyr (98.7%)	0.597 0.673
0521-36	Stellar spectrum of M31 + power-law ($\alpha = -0.5$)	-
0620-52	15 Gyr (67.7%) + 2 Gyr (33.4%)	0.746
0625-35	15 Gyr (45.8%) + power-law ($\alpha = -1.15$, 55.5%)	0.108
0625-53	15 Gyr with E(B-V)=0.3 magnitudes of reddening(104%)	2.59
0915-11	2 Gyr (89.3%) + 0.05 Gyr (10.8%) 10 Gyr (70.0%) + 0.1 Gyr (30.0%)	0.835 0.948
1216+06	10 Gyr (99.4%)	0.617
1246-41	15 Gyr (101.4%)	0.528
1251-12	12.5 Gyr (99.0%)	0.889
1318-43	15 Gyr (102%)	0.836
1333-33	12.5 Gyr (99.9%)	0.939
1514+07	15 Gyr (98.5%)	1.33
1514-24	10 Gyr (17.6%) + power-law ($\alpha = 0.72$, 83.7%)	0.625

either an old elliptical galaxy component or a young stellar component or a combination of the two. Instead, a power-law component is required to gain a good fit to the continuum, with the best fit being the combination of this power-law with a 15 Gyr component ($\chi^2 = 0.108$). However, adequate fits ($\chi^2 \sim 0.1$) are also obtained with the combination of power-law component and elliptical galaxy ages of 5-15 Gyr. Both the [OII] and [OIII] lines are detected and the redshift derived from the fit of the [OII] line ($z=0.525$) has been used in the fitting of the continuum ($z=0.055$ previously quoted by Tadhunter et al. 1993). Interestingly, in this galaxy non-thermal emission has been detected in hard X-rays from SAX (Trussoni et al. 1999). These results are consistent with the relatively large R parameter reported for this source (see

Table 1): 0625-35 has the second largest R parameter in the group, after the well-known BL Lac object 1514-24. As further evidence for the orientation of this object, the R-band imaging paper of Govoni et al. (2000) suggests the presence of a nuclear point source.

0625-53 No obvious UV excess is observed in this galaxy. The best-fitting model, although far from ideal ($\chi^2 = 6.73$), was obtained using a 15 Gyr elliptical galaxy component only. The fit could not be improved by the addition of a young stellar component. However, the fit was improved by reddening the elliptical galaxy component, in order to represent intrinsic reddening within the source. The best fit was obtained with E(B-V)=0.3 and although this final fit is still not ideal ($\chi^2 = 2.59$), the reddening offers a significant improve-

ment. We used a value of the redshift of $z=0.0556$ ($z=0.054$ previously quoted by Tadhunter et al. 1993). No emission lines were detected.

0915-11 (Hydra A) This galaxy has a clear UV excess. It is not possible to gain an adequate fit to the continuum with either an old elliptical galaxy component ($\chi^2 > 14$) or a young stellar component alone ($\chi^2 > 2$). The fit is somewhat improved with the addition of a power-law component although is still far from ideal (e.g. 15 Gyr + power-law with $\alpha = 0.88$ has $\chi^2 = 1.85$). A young stellar component is clearly required and in fact the best-fitting model comprises a 2 Gyr component with a 0.05 Gyr component ($\chi^2 = 0.835$). Acceptable fits ($\chi^2 \sim 0.9$) are also obtained with a 2-15 Gyr component combined with a 0.05-0.1 Gyr component. The presence of a young stellar population in this galaxy has already been discussed by Melnick et al. (1997) and Aretxaga et al. (2001). Melnick et al. state that the prominent Balmer absorption and blue colour of the central disk suggest that massive star formation activity has occurred over at least the past 0.01 Gyr. Aretxaga et al. use their measured Balmer break index and stellar evolutionary tracks to suggest that the last burst of star formation occurred in the last 0.007-0.04 Gyr. In view of these particularly young ages suggested for the most recent burst of star formation, we also attempted to fit to the continuum of HydraA using a 0.01 Gyr component. We find that, we can obtain an acceptable fit if the 0.01 Gyr component is combined with a 2 Gyr component ($\chi^2 = 0.924$). The 2 Gyr + 0.05 Gyr model still remains the best-fit to the continuum although there is little difference between any of the acceptable fits. In conclusion, our results are consistent with the young stellar component identified by Aretxaga et al. We used a value of the redshift of $z=0.0542$ ($z=0.054$ previously quoted by Tadhunter et al. 1993).

1216+06 (3C270) In this galaxy there is no obvious UV excess. The best fit to the continuum is obtained using a redshift of $z=0.00747$ ($z=0.006$ previously quoted by Tadhunter et al. 1993) and an old stellar population (10 Gyr is best, 12.5 Gyr is also acceptable, both with $\chi^2 \sim 0.6$) only. There is no improvement to the fit by the addition of a young stellar component. The [OII] line was marginally detected.

1246-41 (NGC 4696) No obvious UV excess is detected for this galaxy. The best fit to the continuum is with a 15 Gyr elliptical component alone ($\chi^2 = 0.528$). We find no improvement to the fit by the addition of a young stellar component. We detect both the [OII] and [OIII] lines and the redshift derived from the absorption and emission lines is $z = 0.00994$ ($z=0.009$ previously quoted by Tadhunter et al. 1993).

1251-12 (3C 278) No obvious UV excess is detected in this galaxy. A reasonable fit to the continuum is obtained using an old stellar component only (12.5 Gyr is best, 15 Gyr is also acceptable, both with $\chi^2 \sim 0.8$). There is no significant improvement to the fit by the addition of a young stellar component. We detect both the [OII] and [OIII] lines and the redshift derived from the absorption and emission lines is $z = 0.0157$ ($z=0.015$ previously quoted by Tadhunter et al. 1993).

1318-43 (NGC 5090) There is no obvious UV excess in this galaxy. The best fit to the continuum is obtained with just an old stellar population (15 Gyr, $\chi^2 = 0.836$). There is

no significant improvement to the fit with the addition of a young stellar component. The [OII] line is detected and the redshift derived from the absorption lines in the galaxy is $z = 0.0117$ ($z=0.011$ previously quoted by Tadhunter et al. 1993).

1333-33 (IC 4296) There is no obvious UV excess detected in this source. The best fit to the continuum is achieved with just an old stellar population (12.5 Gyr, $\chi^2 = 0.939$). The fit is not improved with the addition of a young stellar component. Only the [OII] line is detected.

1514+07 (3C 317) There is no obvious UV excess in this galaxy. We detect both the [OII] and [OIII] lines and from these deduce an average redshift of $z = 0.034$ ($z=0.035$ previously quoted by Tadhunter et al. 1993). The best fit to the continuum of this galaxy is with a single 15 Gyr component. However, this fit is not ideal ($\chi^2 = 1.33$), probably as a result of differential refraction, since the airmass for the observations of this source was quite high (1.33).

1514-24 (Ap Lib) This is a BL Lac object, classified on the basis of its spectrum and light distribution (e.g. see Disney et al. 74). It is not possible to gain an adequate fit to the continuum with either an old elliptical galaxy component or a young stellar component alone or a combination of the two. Instead a power-law component is clearly required and is the dominant component. We get reasonable fits ($\chi^2 \sim 0.6$) with a 0.05-15 Gyr component combined with a power-law component, with little difference between them. The [OIII] was detected and from this we derived a redshift of $z = 0.0480$.

3.5 Far-Infrared/Starburst Link

In addition to the UV excess, an alternative method for diagnosing the presence of a starburst component in powerful radio galaxies is to use the far-IR excess (e.g. Sanders & Mirabel 1996). However, the heating mechanism for the dust radiating the far-IR emission is controversial: heating by an AGN is a viable alternative to heating by a starburst. In this context, it is interesting to consider whether there is any link between the detection of a young stellar population and the detection of a far-IR excess for the FRI sources in our sample. Recently we found evidence for just such a link in samples of more powerful radio sources (Tadhunter et al. 1996, Wills et al. 2002, Tadhunter et al. 2002).

In Table 2 we show which of the galaxies in our sample are detected in the IRAS ‘all-sky’ survey (as described by Neugebauer et al. 1984) and/or ‘pointed observations’ of desired targets. The pointed observations are the most sensitive observations made with IRAS and for three of our sources such observations exist and have been quoted from Golombek et al. (1988) and Impey & Neugebauer (1988).

The detections were estimated by co-adding scans from the all-sky survey passing within approximately $1.7'$ of the target position. A baseline was fit to each individual scan and the scans were then co-added and analysed. An infrared source observed in a $60 \mu\text{m}$ co-added scan was presumed to be identified with a radio galaxy if the positional agreement was better than $1'$, the peak flux was greater than or close to three times the rms deviation of the residuals after baseline subtraction, and the detection could be confirmed at at least one other wavelength band (either $12 \mu\text{m}$ or $25 \mu\text{m}$) and/or with pointed observations. In the case of a detection, the

flux density was deduced from the best-fitting point source template of the co-added median scans. For the remaining sources, in which no identification with an infrared source could be made, upper limits were derived from three times the median rms deviation of the residuals after baseline subtraction in a 20' region centred on the target position, outside of the central 2.5' signal range. Flux calibration followed the procedure outlined by Young et al. (1988) and conversion of the flux density to a 60 μm luminosity was made assuming an infrared spectral index of -1 (using flux density $f_\nu \propto \nu^{+\alpha}$, as used in Golombek et al. 1988). In Figure 3 we plot the 60 μm luminosity of the sources of the sample against their redshift on a log-log scale.

Using these criteria we find seven clear detections (0521-36, 0620-52, 0625-35, 0915-11, 1318-43, 1333-33, 1514-24) and 2 marginal detections (0453-20, 1246-41). In the case of 0453-20 the detection is only marginal because of a relatively large positional offset between the 60 μm and optical galaxy positions ($\sim 1'$), while in the case of 1246-41 the detection is considered marginal because of relatively poor S/N. Note that, based on the all-sky survey alone, the 60 μm detection of 0915-11 (Hydra A) would be considered marginal, but a flux has also been measured for this source at 60 μm and 100 μm from pointed observations (Golombek et al. 1988), albeit at a low level of accuracy. The pointed and all-sky survey 60 μm fluxes for this source agree within 50%. Therefore, on balance, we regard the detection of this source as secure.

Although the three BL Lac objects in our sample were detected by IRAS, it is likely — given the clear detection of a power-law component at optical wavelengths — that their far-IR fluxes are significantly boosted by non-thermal synchrotron emission. Therefore, we exclude these BL Lacs from the following discussion on the optical starburst/far-IR link.

Our results show that all three of the objects with the best evidence for young stars are either detected or marginally detected by IRAS; the far-IR luminosities of these sources are, in general, significantly larger than those of the sources in which young stars were not detected (see Figure 3). It is also notable that, of the objects definitely not detected by IRAS, none show evidence for young stellar populations. These results point to a link between far-IR and optical starburst activity similar to that found for samples of more powerful radio sources (Wills et al. 2002, Tadhunter et al. 2002). However, more sensitive far-IR observations of the low-luminosity sources will be required to put this link on a firmer footing.

4 DISCUSSION

4.1 UV excess in low power radio galaxies

The presence of a UV excess in powerful radio galaxies compared with quiescent ellipticals has been well known for some time. However, the origin of this excess has been matter of discussion, although its multi-component nature is now clear (Tadhunter et al. 2002). Although the D(4000) parameter has previously been measured in some FRI sources (Owen et al. 1996), this paper represents the first time that the UV excess in low luminosity radio galaxies has been carefully investigated in a complete sample, using both the D'(4000) parameter and the fit to the optical continuum.

Before analysing in detail the results for the low-luminosity sample, it is worth summarising what has been found for powerful radio galaxies (e.g. see Wills et al. 2002 and Tadhunter et al. 2002). For the low redshift sample (Wills et al. 2002), three out of nine of the galaxies show a UV excess which is attributed to a young stellar population and none of these sources require a significant power-law contribution to the excess. This has been found despite the higher radio power and the strong emission lines characteristic of these objects, in contrast to the FRIs studied here. In the higher redshift radio galaxies (Tadhunter et al. 2002), a UV excess is observed in all of the sources of the sample, although the contribution to the UV excess by a young stellar population is found to be a similar fraction of objects ($\sim 30 - 50\%$) to that of the low redshift sample.

4.1.1 Young stellar populations in low-luminosity radio galaxies

From the D'(4000) parameter we found that 5 (0453-20, 0620-52, 0625-35, 0915-11, 1514-24) out of the 13 observed galaxies have a value indicating a possible additional blue component. However, only by performing the fit to the continuum are we able to really identify the nature of this component. A young stellar population component (0.05 - 2 Gyr) gives a substantial contribution to the UV excess in three of these five galaxies (0453-20, 0620-52 and 0915-11). For the remaining two, the dominant additional component is a power-law. The latter is expected in the case of 1514-24 since this is a well known BL Lac object. However, as discussed in the notes, the second object, 0625-35, also appears to have the characteristics of a BL Lac. This trend is also confirmed for the third BL Lac in the sample, 0521-36, for which a power-law component was found from data in the literature.

Excluding the BL Lacs, three out of eleven galaxies in our sample show a significant contribution from a young stellar component. This fraction is similar to that found for powerful FRII radio galaxies ($\sim 30\%$; see Wills et al. 2002 and Tadhunter et al. 2002). Thus, *the fraction of galaxies with a young stellar population component does not seem to depend on the power of the galaxies*. Assuming that the radio activity is triggered by a merger, which also triggered a starburst, then this perhaps indicates that there is no major difference in the origin, 'triggering' and time-scale of the activity in both kinds of radio sources.

4.1.2 The power-law component

Another interesting result of this study, is that we only find definite evidence for the presence of a power-law component in the three BL Lac objects. From our data, therefore, it appears that *a power-law component is not required in the fit to the continuum of the host galaxy of FRI radio sources*.

This result is intriguing since, at first sight, it appears to be in disagreement with recent HST results. As already described in §1, optical compact cores have been found in a large fraction of galaxies hosting FRI radio sources (e.g. Capetti & Celotti 1999). The correlation between their flux and the flux of the radio cores for FRI/BL Lacs indicates that these optical cores are due to optical synchrotron radiation, supporting the similarities between FRI and BL Lacs

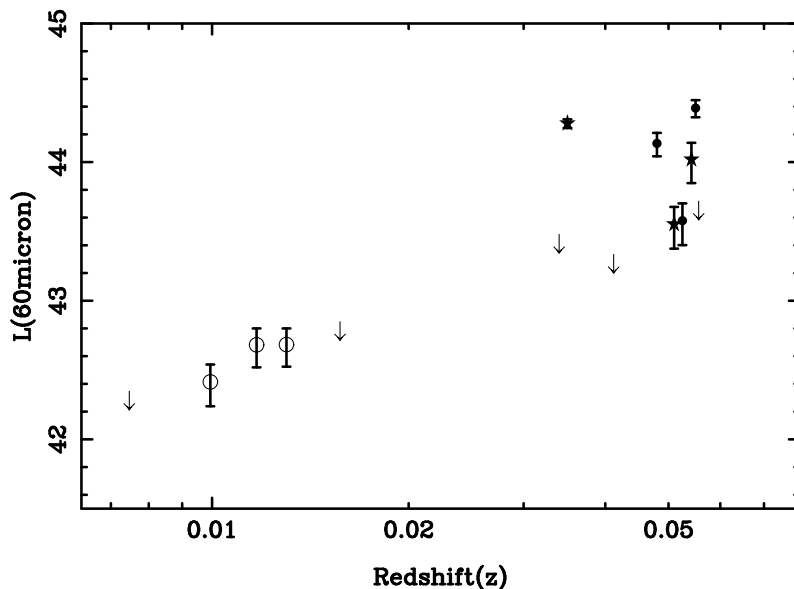


Figure 3. The 60 μm luminosity of the sources of the sample plotted against redshift presented as a log-log plot. The filled star symbols represent those sources showing evidence of young stars and the filled circles represent the BL Lac objects. The sources which show no UV excess but are detected by IRAS are represented by open circles and those which show no UV excess and are also not detected by IRAS are represented by arrows indicating the upper limit to the 60 μm luminosity.

as predicted by unified schemes. Given the low amount of obscuration predicted (e.g. see Chiaberge et al. 1999, Morganti et al. 2001) we would therefore also expect a power-law component in a number of FRI radio galaxies. However, the cores detected by the HST are actually quite weak (typically 10^{-17} to 10^{-16} $\text{erg cm}^{-2} \text{s}^{-1} \text{\AA}^{-1}$) and therefore, they represent only a minor contribution (i.e. only a few percent or less) to the optical flux for a typical ground-based extraction aperture. The typical extraction aperture used here (2×7 arcsec), depending on the redshift of the individual source, corresponds to approximately several kiloparsecs. On this scale the contribution of the host galaxy represents a major fraction.

4.2 Radio-optical correlation: is there a difference between FRIs and IIs?

By subtracting the continuum from the spectra of the galaxies we have detected emission lines in six galaxies where previously only upper limits were available. This allows us to further investigate the correlation between radio power and emission line luminosity. With all the available data on the 2Jy sample we have constructed separate correlations for 5 GHz radio power versus the luminosities of [OII] and [OIII] emission lines respectively (see Figure 4). In this way, we can extend the work carried out by Tadhunter et al. (1998) to the low radio power regime.

In Figure 4, for the higher redshift range, we have taken all the radio galaxies from the 2Jy sample described in Tadhunter et al. (1998) with $z > 0.1$ (a complete sample consisting of mainly FRII sources but also some compact radio sources and FRI/FRII transition sources, including 1648+05 (Her A)). For the lower redshift range, we have included all the sources from our complete sample presented here and all the radio galaxies with $z < 0.1$ from Tadhunter et al.

(1993: this comprises a complete sample of FRIIs only since the FRIs/BL Lacs with $z < 0.1$ are already included in our sample). In this way, we are actually comparing detections and upper limits resulting from spectra of similar quality for both low-power and high-power radio sources.

The analysis of the correlations has been carried out using the ASURV Rev 1.2 package (Lavalley, Isobe & Feigelson 1992, Isobe, Feigelson & Nelson 1986, Feigelson & Nelson 1985) in order to take into account the upper limits. In our analysis, the 5 GHz radio power was always considered as the independent variable. The parameters obtained and the significance of the correlations are summarized in Table 4 including the probability that the two quantities are independent. Note that, although at 5 GHz the BL Lac sources will probably have a large component of beamed flux, the results of our correlations (within the errors) are not affected by the removal of these sources from the data entirely and therefore this effect is not significant.

For all available data on the 2Jy sample, we find that there is a clear correlation between the radio power and both the [OIII] and [OII] line luminosities. The presence of a correlation between line luminosity and radio power is already well known from a number of studies (e.g. see Baum & Heckman 1989a,b, McCarthy 1988, Morganti, Ulrich & Tadhunter 1992, Rawlings et al. 1989, Tadhunter et al. 1998). However, in the previous studies, the correlation was mainly investigated using the luminosity of only *one* emission line (usually either [OIII] or $H\alpha$). In the single previous case where two lines were used ([OIII] and [OII], Tadhunter et al. 1998) the sample was limited to powerful radio galaxies ($z > 0.1$). Our data, therefore, allows a significant expansion on previous results.

From the parameters of the correlations listed in Table 4, it appears that [OIII] and [OII] follow correlations with two marginally different slopes, with the latter showing a

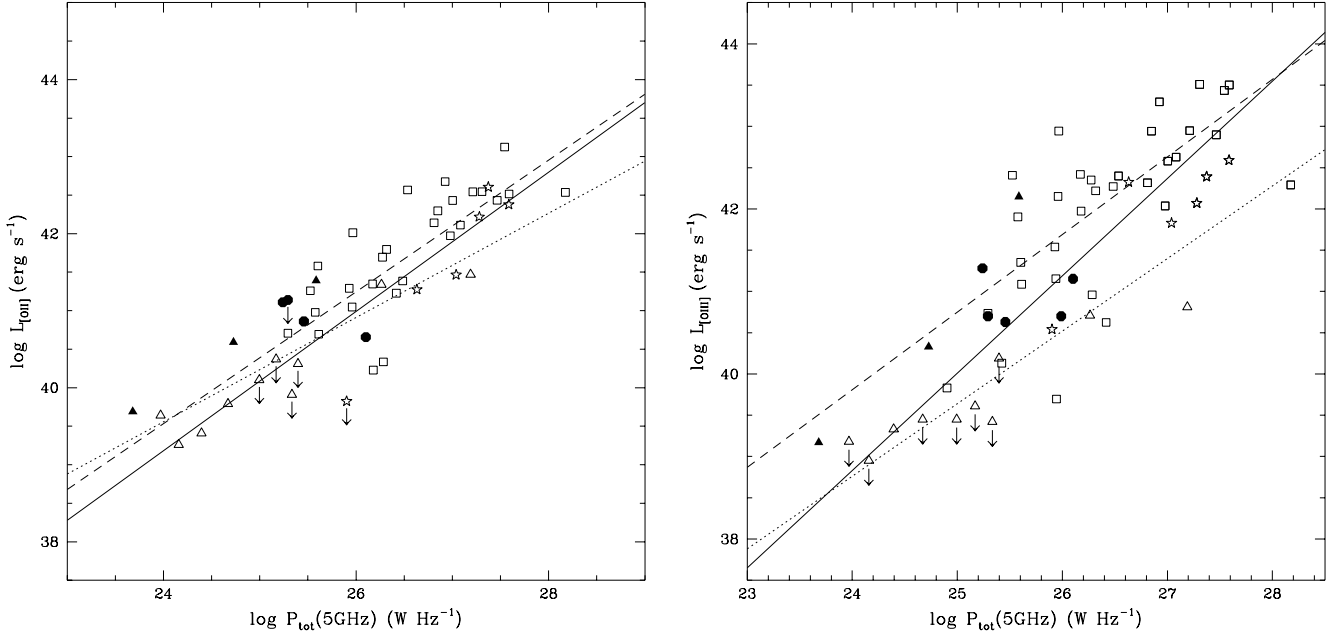


Figure 4. The correlation between radio power versus [OII] (left) and [OIII] (right) emission line luminosities for the 2Jy sample of radio galaxies (see text for further details). The objects are classified according to their radio properties as follows: open squares - FRII; open triangles - FRI; open stars - compact steep spectrum (CSS) radio sources; filled circles - BL Lac objects including two additional objects (1807+69 ($\log P_{tot} = 25.2$, $\log L_{[OII]} = 41.1$, $\log L_{[OIII]} = 41.3$) and 2200+42 ($\log P_{tot} = 26.0$, $\log L_{[OII]}$ not available, $\log L_{[OIII]} = 40.7$) from Stickel, Fried & Kuehr (1993); filled triangles - uncertain radio classifications. In both plots, the solid line represents the best fit to all data in the sample, the short-dashed line represents the fit to the FRI and BL Lac objects and the long-dashed line is the fit to the FRII and CSS objects. Details of the fitting procedure and resulting fits are described in the text and in Table 4.

Table 4. Correlation analysis for the 2Jy sample shown in Figure 4. The analysis has been performed separately for the full sample (see solid line in Figure 4), the FRI and BL Lac objects (see short-dashed line) and the FRII and CSS objects (see long-dashed line). The parameters of the fits are presented and the final column gives the significance level of the correlation (i.e. the percentage probability that the correlations could arise by chance, see text for more details).

Correlation	Sample	Best fit		
		Slope	Intercept	Coeff. %
$\log P_{5\text{GHz}}$ vs $\log L_{[OIII]}$	All	1.18 ± 0.11	10.51 ± 2.83	<0.01
	FRII + CSS	0.94 ± 0.15	17.25 ± 3.86	<0.01
	FRI + BL Lac	0.88 ± 0.27	17.64 ± 6.80	0.1
$\log P_{5\text{GHz}}$ vs $\log L_{[OII]}$	All	0.91 ± 0.07	17.35 ± 1.91	<0.01
	FRII + CSS	0.86 ± 0.12	19.01 ± 3.20	< 0.01
	FRI + BL Lac	0.69 ± 0.14	22.93 ± 3.51	0.4

somewhat flatter slope. The two correlations also have a different scatter: the correlation with [OII] has a much smaller scatter than that of the [OIII]. This was already noted for the sample of mostly powerful radio galaxies studied by Tadhunter et al. (1998). The explanation of this result is provided by the photoionization model, where the [OIII] lines are more sensitive to variation in the ionising continuum.

It is interesting to investigate from the new data whether the correlations of the radio power versus emission line luminosity are different for low-power FRI and high-power FRII galaxies. This is an important question since it may point to different mechanisms for ionising the gas in the two groups of galaxies (see Baum et al. 1995). When

we split the sample into FRI and FRII radio morphologies, we find that (see Figure 4 and Table 4), *FRIIs follow the correlation between line luminosity and radio power with a similar slope to that found for the FRIIs*. The significance of the correlations (in particular between [OII] luminosity and radio power) is, however, lower for the FRIIs than for the FRIIs.

The slope found in the [OII] correlation is consistent (within the errors) with the result obtained by Morganti et al. (1992) using $H\alpha$ lines for a sample of low-luminosity radio galaxies taken from the B2 sample and a sample of 3C powerful radio galaxies (from Baum & Heckman 1989a,b). It is, however, much steeper than the slope derived by Zirbel &

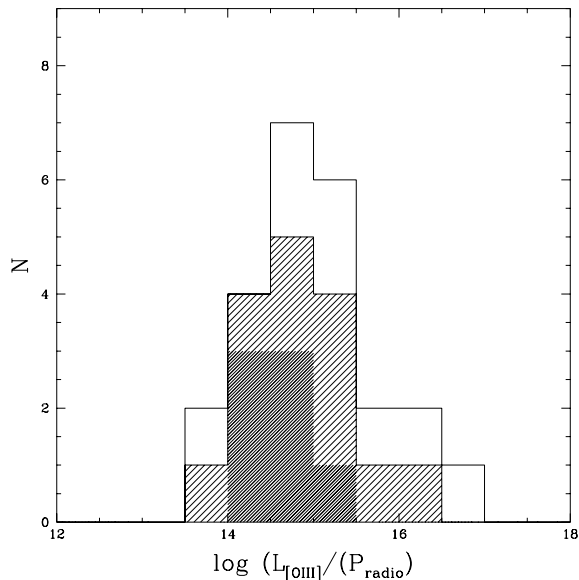


Figure 5. Distribution of the ratio $L_{[OIII]}/P_{radio}$ for the 2Jy sample. FRIs are shown as large dashed and the upper limits for the FRIs are shown as narrow dashed; the rest of the histogram represents the FRIIs. See text for more details.

Baum (1995) for a large but heterogeneous sample of objects collected from the literature (mainly using $H\alpha + [NII]$ emission line luminosities). It is likely that this difference is due to the uncertainties involved in their fitting of a combination of samples selected using different criteria which includes the mixing of emission lines ([OIII] is used when $H\alpha$ is unavailable), the mixing of radio frequencies (5GHz measurements are used when no good 408 MHz observations are available) and, most importantly, the inclusion of a number of sources where no emission line luminosity information is available. This latter issue has the effect of introducing an emission line flux density limit since the fainter sources (mostly FRIs) are more likely to go undetected. Since the sample is already radio flux density limited, this results in difficulty interpreting any correlation observed between radio flux and emission line luminosity, particularly for the FRIs. In contrast, our sample, the Morganti et al. sample and the Baum & Heckman samples mentioned above are all based on homogeneous data and result in consistent measurements of the slope.

Despite the similarities mentioned above, an offset is evident in the [OIII] luminosity versus radio power plot, between the correlation for FRIs and FRIIs. This can be seen even more clearly in the histogram of Figure 5 showing the ratio between the optical luminosity and the radio power. Here we compare all the FRIs from our sample with all FRIIs from Tadhunter et al. (1993) within the same redshift range (i.e. $z < 0.06$). The difference is highly significant (with a probability of 3% that the two distributions are similar, estimated using ASURV). The observed offset confirms the results obtained by Zirbel & Baum (1995) and Baum et al. (1995) since the FRI galaxies, for a given radio power, have systematically lower optical line luminosity than their powerful cousins.

In summary, we find that the low-luminosity FRI radio

galaxies follow a correlation between the luminosity of the lines (both in [OII] and in [OIII]) and their radio power, and that the slope of these correlations is not too dissimilar from the one found for FRIIs. This result supports the idea that in FRIs, as in FRIIs, nuclear UV radiation is responsible for the ionization of the gas around the AGN. This conclusion is quite different from that reached by Baum et al. (1995): their work suggests that two different mechanisms are responsible for the ionization of the lines, on the basis of their finding of a large difference in slope for FRIs compared with FRIIs. However, it is indeed the case that FRIs have a systematically lower line luminosity (for their radio power) compared with FRIIs, although this is mainly the case for the [OIII] luminosity. Interestingly, at the transition between FRI and FRII (around $10^{25.5}$ at 5GHz) the [OIII] luminosities seem to become suddenly stronger and show a ‘step’ in their distribution, a feature which is not detected in [OII] (see Figure 4). A possible explanation of this is that, based on the photoionization models, [OIII] is much more sensitive to changes in the ionising continuum than [OII]. Below a critical ionization parameter of $U \sim 10^{-3}$ the photoionization models show that the correlation between the [OIII] luminosity and the ionization continuum steepens (from 1.2 to 3.3). Thus, if the ionising continuum luminosity were to be significantly less for the FRIs than the FRIIs, this would be much more apparent in [OIII] than [OII] - perhaps leading to the ‘step’ seen in the [OIII] plot.

Thus, the differences between FRIs and FRIIs could reflect a change to a different mode of accretion: advective low efficiency flow (e.g. see Rees et al. 1982) for FRIs and standard optically thick accretion disks (e.g. see Véron & Véron-Cetty 2000) for FRIIs. Since the latter would be expected to produce ionising photons more efficiently, this is qualitatively consistent with what we observe, and may also be consistent with the failure to detect broad lines in FRIs (e.g. Capetti et al. 2002).

4.3 FRI, BL Lacs and unified schemes

According to the unified schemes for radio loud objects, FRIs are believed to be the parent population of BL Lac objects (Urry & Padovani 1995). If this is the case, we would expect the luminosity of the emission lines in the two groups of objects to be similar. This is because the emission lines are not expected to suffer from any beaming effect.

This important test for the unified schemes has already been carried out for FRIIs and radio-loud quasars. In this case, differences were found in the luminosity of the [OIII] lines (with quasars showing emission line luminosities typically 5-10 times higher than, otherwise similar, FRIIs; Jackson & Browne 1990) while the luminosities of the [OII] lines were found to be similar in the two groups (Hes, Barthel & Fosbury 1996). This result has been explained in terms of obscuration from the circumnuclear torus which affects high ionization lines more than the low ionization lines since the former are believed to originate closer to the nucleus.

In the case of the FRIs and BL Lacs, if we are to assume that no significant absorption occurs in the FRI sources, then we should expect no difference between the [OII] and [OIII] emission line luminosities. However, the question of whether obscuration exists in FRIs is still a matter of discussion (Chiaberge et al. 1999, Morganti et al. 2001, Chiaberge

et al. 2002, Hardcastle et al. 2002). For example, recent work by Chiaberge et al. (2002) has suggested that there is clear evidence of nuclear absorption in some FRI sources but not by a ‘standard’ torus-like structure. Instead they suggest that the moderate amount of absorption observed might be accounted for either by extended kpc scale dust lanes or by ~ 100 pc scale dusty disks.

Urry & Padovani (1995) have already attempted a comparison between these two groups, using data available in the literature. Interestingly, their results tentatively suggest an apparent difference between the [OIII] luminosities of BL Lacs and FRIs, with the former stronger than the latter. However, their comparison uses data from different samples and the FRI fluxes may well be underestimated due to small slits and contamination from a strong stellar continuum. To determine if this [OIII] difference is really significant, we now repeat this study using our complete sample, which consists of high quality optical spectra for which the continua have been accurately subtracted. Using ASURV, we have estimated both the mean of the distributions as well as the probability that the two distributions are drawn from the same parent population. The statistical tests used within ASURV to compare the distributions are Gehan’s generalised Wilcoxon test, the Logrank test, the Peto-Peto test and the Peto-Prentice test. These tests are generalisations of standard techniques based on ranking the data values and comparing the distributions of the ranks. Consistent results were obtained for all the tests which support the tentative suggestion by Urry & Padovani (1995) that the [OIII] luminosity of the BL Lacs is higher than the FRIs. Since our sample only contains three BL Lacs, we have also repeated these tests including two additional objects (1807+69 and 2200+42) from the compilation of Stickel et al. (1993), which contains sources of a similar range in radio power to our sources. These additional two sources are the only two from the sample of Stickel et al., together with ApLib, to have $z < 0.150$ and line luminosity data available. We find that similar results and conclusions can be drawn with the addition of these two objects and the distributions of luminosity of the emission lines and radio power for the FRI and BL Lac sources (including the Stickel sources) are presented in Figure 6. In Table 5 we summarize the results of the statistical tests performed within ASURV. Note that this gives the typical values obtained for the different tests used within ASURV (including the Stickel sources) and is in good agreement with the results obtained without the addition of the Stickel objects.

From these results it appears that *while the difference between FRIs and BL Lacs is marginal for the [OII] line luminosities, there is a significant difference in the luminosity of the [OIII] lines*: The [OIII] luminosity of the BL Lacs is higher (40.840 ± 0.156) than the FRIs (39.509 ± 0.213). This is an interesting result in view of the current debate on obscuration in FRIs, since this does indeed suggest that a significant amount of obscuration exists. Of course our result should be taken with some care, since it has been derived from a small sample. Nevertheless, it is in agreement with the tentative suggestion made by Urry & Padovani (1995).

An alternative explanation to obscuration that must be investigated is the possibility that some selection effect has been introduced in the BL Lac sample. We therefore looked at the distribution of total radio power for FRI and BL Lacs

Table 5. Comparison of the distributions of the BL Lac sources and FRI sources for the 14 radio galaxies in our sample plus two additional BL Lac objects (1807+69 and 2200+42) taken from Stickel et al. (1993). The final column gives the percentage probability that the two distributions are drawn from the same parent population. See text for more details.

Sample	Mean	Probability (%)
[OII] BL Lacs	40.820 ± 0.096	
FRI	39.960 ± 0.235	~ 6
[OIII] BL Lacs	40.840 ± 0.156	
FRI	39.509 ± 0.213	~ 0.8
Radio BL Lacs	25.260 ± 0.236	
FRI	25.220 ± 0.322	70

(see Figure 6 and Table 5) but no difference was found. In fact, since the radio powers of three of the BL Lacs are dominated by the core emission, this suggests that the BL Lacs in our sample have much lower extended radio powers than the total powers displayed in Figure 4. Therefore, the BL Lac sources should be compared with the FRI sources in the sample at the lower end of the emission line luminosity and radio power distribution. This strengthens our finding that the BL Lacs have higher [OIII] luminosities than the FRIs in the sample.

Another possibility is that *FRIs do not represent the parent population of all BL Lacs*. The suggestion that the simple picture of the unified scheme is probably not adequate has already been made (Kollgaard et al. 1992, Murphy, Browne & Perley 1993) and it has also been put forward that weak-lined FRIs could be associated with BL Lacs (and not with quasars; Jackson & Wall 1999).

5 CONCLUSIONS

In a complete sub-sample of 13 low-luminosity radio galaxies, we find that 5 show a UV excess and, in 3 cases, this excess appears to be due to the presence of young stars. The remaining two sources which show a UV excess are BL Lac objects. Excluding the BL Lac objects, we therefore find that $\sim 30\%$ of our low-luminosity sample show evidence for a young stellar population. Since this is similar to the fraction found for powerful FRII radio galaxies, we suggest that the proportion of galaxies with young stars does not depend on the power of the galaxies. Furthermore, our modelling also suggests that a power-law component is not required in the fit to the continuum of the host galaxy of FRI radio sources.

We find that the three objects which show evidence for young stars are either detected or marginally detected by IRAS and are among the highest $60 \mu\text{m}$ luminosity sources in the sample. Of the objects definitely not detected by IRAS, none show evidence for young stellar populations. This suggests a link between far-IR and optical starburst activity similar to that found for samples of more powerful radio sources.

On studying the correlations between radio power and the [OIII] and [OII] line luminosities of the 2Jy sample we find that the FRI sources follow the correlations with a sim-

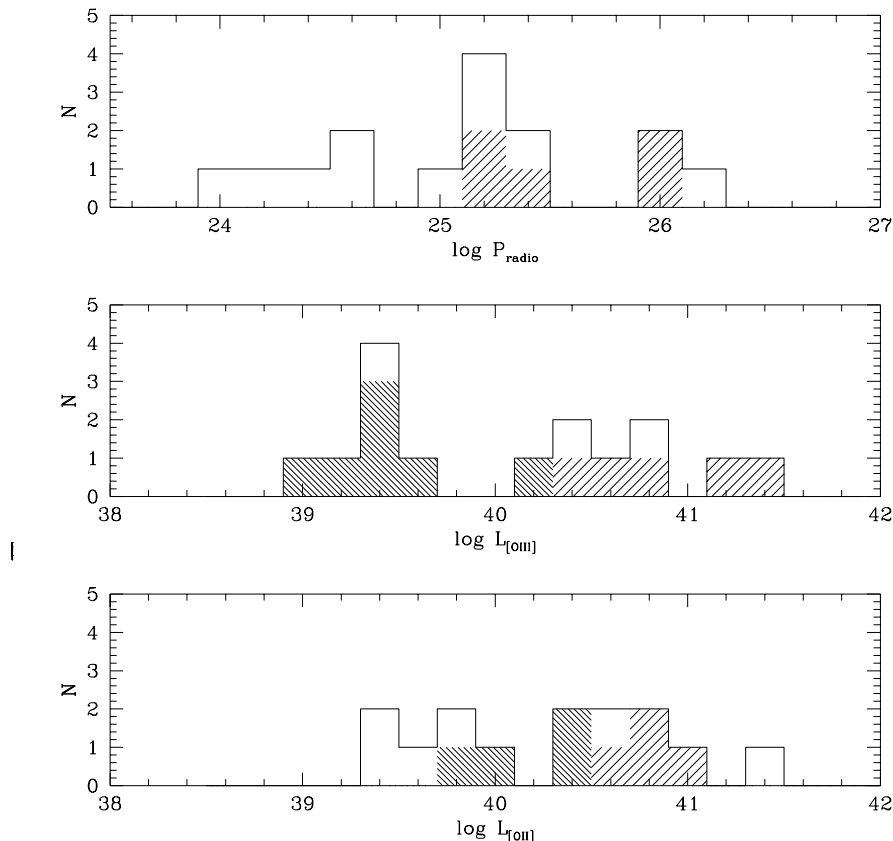


Figure 6. Distribution of total radio power, [OIII] and [OII] line luminosities for the FRI and BL Lac sources in our sample, plus two additional BL Lac objects (1807+69 and 2200+42) taken from Stickel et al. (1993). The BL Lacs are shown as large dashed and the upper limits for the FRIs are shown as narrow dashed; the rest of the histogram represents the remaining FRIs.

ilar slope to that found for the FRIIs. This result supports the idea that in FRIs, as in FRIIs, nuclear UV radiation is responsible for the ionization of the gas around the AGN.

Our investigation into the luminosity of the emission lines in the FRI and BL Lac sources has shown that there is a significant difference in the [OIII] line luminosities of the two groups, whilst the difference in [OII] is marginal. A similar result has also been found for FRIIs and radio-loud quasars, which has been explained in terms of obscuration of the high ionization lines which originate closer to the nucleus. To explain the same result in our low-luminosity sample we must either invoke some kind of obscuration model or conclude that the two groups cannot actually be unified.

Acknowledgments

We acknowledge the expert advice and assistance of the scientific support staff and the data analysis team at the Infrared Processing and Analysis Facility (IPAC). We also acknowledge the data reduction package FIGARO provided by the Starlink Project which is run by CCLRC on behalf of PPARC. This research has made use of the NASA/IPAC Extragalactic Database (NED) which is operated by the Jet Propulsion Laboratory, California Institute of Technology, under contract with the National Aeronautics and Space

Administration. KAW is supported by a Dorothy Hodgkin Royal Society Fellowship.

REFERENCES

- Aretxaga I., Terlevich E., Terlevich R., Cotter G., Diaz A. I., 2001, MNRAS, 325, 636
 Baum S., Heckman T., 1989a, ApJ, 336, 681
 Baum S., Heckman T., 1989b, ApJ, 336, 702
 Baum S.A., Zirbel E.L., O’Dea C.P. 1995 ApJ, 451, 88
 Boisson C., Cayatte V., Sol H., 1989, A&A, 211, 275
 Bruzual A. G., 1983, ApJ, 273, 105
 Capetti A., Celotti A., 1999, MNRAS, 304, 434
 Capetti A., Celotti A., Chiaberge M., de Ruiter H. R., Fanti R., Morganti R., Parma P., 2002, A&A, 383, 104
 Chiaberge M., Capetti A., Celotti A., 1999, A&A, 349, 77
 Chiaberge M., Macchetto F. D., Sparks, W. B., Capetti A., Allen M. G., Martel A. R., 2002, ApJ, 571, 247
 Danziger I.J., Fosbury R.A.E., Goss W.M., Ekers R.D., 1979, MNRAS, 188, 415
 Dickson R. C., Tadhunter C. N., Shaw M. A., Clark N., Morganti R., 1995, MNRAS, 273, L29
 Disney M. J., Peterson B. A., Rodgers A. W., 1974, ApJ, L79
 Fanaroff B. L., Riley J. M., 1974, MNRAS, 167, 31P
 Feigelson E.D., Nelson P.I., 1985, ApJ, 293, 192
 Golombek D., Miley G. K., Neugebauer G., 1988, AJ, 95, 26

- Govoni F., Falomo R., Fasano G., Scarpa R., 2000, *A&A*, 353, 507
- Hardcastle M. J., Worrall D. M., Birkinshaw M., Laing R. A., Bridle A. H., 2002, astro-ph 0203374
- Hes R., Barthel P.D., Fosbury R.A.E., 1996, *A&A*, 313, 423
- Impey C.D., Neugebauer G., 1988, *AJ*, 95, 307
- Isobe T., Feigelson E.D., Nelson P.I., 1986, *ApJ*, 306, 490
- Jackson C. A., Wall J. V., 1999, *MNRAS*, 304, 160
- Jackson N., Browne I. W. A., 1990, *Nat*, 343, 43
- Kollgaard R. I., Wardle J. F. C., Roberts D. H., Gabuzda D. C., 1992, *AJ*, 104, 1687
- Lavalley M., Isobe T., Feigelson E., 1992, *Astronomical Data Analysis Software and Systems I*, A.S.P. Conference Series, Vol. 25, Diana M. Worrall, Chris Biemesderfer, and Jeannette Barnes, eds., p. 245.
- Leitherer C. et al., 1996, *PASP*, 108, 996
- McCarthy P. J., 1989, PhD Thesis, California Univ., Berkeley.
- Melnick J., Gopal-Krishna, Terlevich R., 1997, *A&A*, 318, 337
- Morganti R., Ulrich M.-H., Tadhunter C.N. 1992, *MNRAS* 254, 546
- Morganti R., Killeen N. E. B., Tadhunter C.N. 1993, *MNRAS*, 263, 1023
- Morganti R., Oosterloo T., Tadhunter C. N., Aiudi R., Jones P., Villar-Martin M., 1999, *A&AS*, 140, 355
- Morganti R., Oosterloo T., Tadhunter C. N., van Moorsel G., Killeen N., Wills K. A., 2001, *MNRAS*, 323, 331
- Murphy D. W., Browne I. W. A., Perley R. A., 1993, *MNRAS*, 264, 298
- Neugebauer G., et al., 1984, *ApJ*, 278, L1
- Owen F. N., Ledlow M. J., Keel W. C., 1996, *AJ*, 111, 530
- Rawlings S., Saunders R., Eales S.A., Mackay C.D., 1989, *MNRAS*, 240, 701
- Rees M.J., Phinney E.S., Begelman M.C., Blandford R.D., 1982, *Nature*, 295, 17
- Robinson T. G., Tadhunter C. N., Axon D. J., Robinson A., 2000, *MNRAS*, 317, 922
- Salpeter E. E., 1955, *ApJ*, 121, 161
- Sanders D. B., Mirabel I. F., 1996, *ARA&A*, 34, 749
- Schlegel D. J., Finkbeiner D. P., Davis M., 1998, *ApJ*, 500, 525
- Seaton M. J., 1979, *MNRAS*, 187, 73P
- Stickel M., Fried J. W., Kuehr H., 1993, *A&AS*, 98, 393
- Tadhunter C. N., Morganti R., di Serego-Alighieri S., Fosbury R. A. E., Danziger I. J., 1993, *MNRAS*, 263, 999
- Tadhunter C. N., Dickon R. C., Shaw M. A., 1996, *MNRAS*, 281, 591
- Tadhunter C. N., Morganti R., Robinson A., Dickson R., Villar-Martin M., Fosbury R. A. E., 1998, *MNRAS*, 298, 1035
- Tadhunter C. N., Dickson R. C., Morganti R., Robinson T. G., Wills K. A., Villar-Martin M., 2002, *MNRAS*, In Press
- Trussoni E., Vagnetti F., Massaglia S., Feretti L., Parma P., Morganti R., Fanti R., Padovani P., 1999, *A&A*, 348, 437
- Urry C.M., Padovani P. 1995 *PASP* 107, 715
- Venturi T., Morganti R., Tzioumis T., Reynolds J., 2000, *A&A* 363, 84
- Verdoes Kleijn G.A., Baum S.A., de Zeeuw P.T., O'Dea C.P., 2002, *AJ*, 123, 1334
- Véron-Cetty, M.P., Véron P., 2000, *A&AR*, 10, 81
- Wills K.A., Tadhunter C. N., Robinson T. G., Morganti R., 2002, *MNRAS*, 333, 211
- Young E. T., Neugebauer G., Kopan E. L., Conrow T. P., Rice W. L., Gregorich D. T., 1988, *A Users Guide to IRAS Pointed Observation Products*, IPAC preprint PRE-008N
- Zirbel E.L., Baum S.A., 1995, *ApJ*, 448, 521